Suppression of high-p_T hadrons in Pb+Pb collisions at energies available at the CERN Large Hadron Collider

Xiao-Fang Chen,[1] Tetsufumi Hirano,[2,3] Enke Wang,[1] Xin-Nian Wang,[1,3] and Hanzhong Zhang[1]

[1]*Institute of Particle Physics, Huazhong Normal University, Wuhan 430079, China*

[2]*Department of Physics, The University of Tokyo, Tokyo 113-0033, Japan*

[3]*Nuclear Science Division, MS 70R0319, Lawrence Berkeley National Laboratory, Berkeley, California 94720, USA*

(Received 23 March 2011; revised manuscript received 26 April 2011; published 6 September 2011)

The nuclear modification factor $R_{AA}(p_T)$ for large transverse momentum pion spectra in Pb+Pb collisions at $\sqrt{s} = 2.76$ TeV is predicted within the next-to-leading order perturbative QCD parton model. The effect of jet quenching is incorporated through medium-modified fragmentation functions within the higher-twist approach. The jet transport parameter that controls medium modification is proportional to the initial parton density, and the coefficient is fixed by data on the suppression of large-p_T hadron spectra obtained at the BNL Relativistic Heavy Ion Collider. Data on charged hadron multiplicity $dN_{\rm ch}/d\eta = 1584 \pm 80$ in central Pb+Pb collisions from the ALICE experiment at the CERN Large Hadron Collider are used to constrain the initial parton density both for determining the jet transport parameter and the 3 + 1 dimensional (3 + 1D) ideal hydrodynamic evolution of the bulk matter that is employed for the calculation of $R_{\rm PbPb}(p_T)$ for neutral pions.

DOI: 10.1103/PhysRevC.84.034902 PACS number(s): 12.38.Mh, 24.85.+p, 25.75.−q

I. INTRODUCTION

One important evidence for the formation of strongly coupled quark-gluon plasma (QGP) [1–4] in high-energy heavy-ion collisions at the BNL Relativistic Heavy Ion Collider (RHIC) is the observation that the produced dense matter is opaque to a propagating parton due to jet quenching [5] which suppresses not only the single inclusive hadron spectra at large transverse momentum [6,7] but also back-to-back high-p_T dihadron [8] and γ-hadron correlation [9–11]. These observed jet quenching patterns in heavy-ion collisions at RHIC can be described well by perturbative QCD (pQCD) parton models [12–21] that incorporate parton energy loss [22,23] as it propagates through dense matter. Since the energy loss or medium modification of the effective jet fragmentation functions depends on the space-time profile of parton density in the medium, any systematic and qualitative extraction of the properties of the medium through phenomenological study of jet quenching has to take into account the dynamical evolution of the bulk matter [24–26]. The initial condition for the evolution of bulk matter is either provided by model calculations or experimental data on the total charged hadron multiplicity. Without any experimental data on hadron production in heavy-ion collisions at the Large Hadron Collider (LHC), all predictions for jet quenching [27] have to rely on theoretical or phenomenological models on the initial condition for bulk matter production and evolution. However, these theoretical and phenomenological predictions for the bulk hadron production [27] vary by almost a factor of 2 and, consequently, lead to the same amount of uncertainties in the predictions for suppression of large transverse momentum hadrons in heavy-ion collisions at the LHC.

Recently, the ALICE experiment at LHC published the first experimental data on the charged hadron multiplicity density at midrapidity in central Pb+Pb collisions at $\sqrt{s} = 2.76$ TeV [28]. The measured $dN_{\rm ch}/d\eta = 1584 \pm 4({\rm stat.}) \pm 76({\rm sys.})$ for the top 5% central Pb+Pb collisions is larger than most theoretical predictions, especially those from the so-called color-glass-condensate models [28]. Such an unexpected large hadron multiplicity will have important consequences on theoretical predictions for jet quenching in Pb+Pb collisions at LHC energies. The predictions for single and dihadron suppression in the most central Pb+Pb collisions at $\sqrt{s} = 5.5$ TeV by Wang, Wang, and Zhang [27] relied on the modified HIJING calculation [29] of the charged hadron multiplicity in heavy-ion collisions at the LHC. The modification has now been incorporated into HIJING 2.0 version [30] of the original HIJING1.0 model [31]. The new HIJING2.0 results [30,32] agree well with the first ALICE data [28] within experimental errors and theoretical uncertainty which is controlled mainly by the uncertainty in nuclear shadowing of gluon distribution in nuclei.

With the first ALICE data [28] providing more stringent constraints on the theoretical uncertainty in the bulk hadron production, we would like to revisit the predictions on suppression of single inclusive hadron spectra at large p_T in heavy-ion collisions at LHC. Moreover, we will use the 3 + 1 dimensional (3 + 1D) ideal hydrodynamic model for a more realistic description of the bulk matter evolution whose initial conditions at LHC are also much better constrained by the first ALICE data.

The rest of the paper is organized as follows. In the next section, we will provide a brief overview of the pQCD parton model for single inclusive hadron spectra and the high-twist (HT) approach to the medium-modified fragmentation functions. In Sec. III, we will give a brief description of the 3 + 1D ideal hydrodynamic model for the bulk evolution with the initial condition provided by the HIJING2.0 model and further constrained by the first ALICE data. In Sec. IV, we present predictions for the nuclear modification factor $R_{AA}(p_T)$ for neutral pions in Pb+Pb collisions at LHC energy $\sqrt{s} = 2.76$ TeV$/n$ and discuss the first LHC data for the charged hadrons from ALICE. We give a summary and discussion in Sec. V.

II. pQCD PARTON MODEL AND MEDIUM-MODIFIED FRAGMENTATION FUNCTIONS

We will employ the next-to-leading order (NLO) pQCD parton model for the initial jet production spectra, which has been shown to work well for large-p_T hadron production in high-energy nucleon-nucleon collisions [33]. We use the same factorized form for the inclusive particle production cross section in $A + B$ heavy-ion collisions, which can be expressed as a convolution of parton distribution functions inside the nuclei (nucleons), elementary parton-parton scattering cross sections and effective parton fragmentation functions,

$$\frac{d\sigma^h_{AB}}{dy\, d^2p_T} = \sum_{abcd} \int d^2b\, d^2r\, dx_a\, dx_b t_A(\mathbf{r}) t_B(|\mathbf{r}-\mathbf{b}|) \times f_{a/A}(x_a,\mu^2) f_{b/B}(x_b,\mu^2) \frac{d\sigma}{d\hat{t}}(ab\to cd) \times \frac{\widetilde{D}_{h/c}(z_c,\mu^2,E,b,r)}{\pi z_c} + O(\alpha_s^3), \tag{1}$$

where $d\sigma(ab \to cd)/d\hat{t}$ are elementary parton scattering cross sections at leading order (LO) α_s^2. The average over the azimuthal angle of the initial jet is implicitly implied in the above equation since we focus on the azimuthal integrated single inclusive hadron cross section. The NLO contributions include $2 \to 3$ tree level contributions and 1-loop virtual corrections to $2 \to 2$ tree processes [33]. The nuclear thickness function is normalized to $\int d^2r t_A(\mathbf{r}) = A$. The nuclear parton distributions per nucleon $f_{a/A}(x_a, \mu^2, \mathbf{r})$ are assumed to be factorized into the parton distributions in a free nucleon $f_{a/N}(x, \mu^2)$ and the nuclear shadowing factor $S_{a/A}(x, \mu^2, \mathbf{r})$,

$$f_{a/A}(x,\mu^2,\mathbf{r}) = S_{a/A}(x,\mu^2,\mathbf{r})\left[\frac{Z}{A} f_{a/p}(x,\mu^2) + \left(1-\frac{Z}{A}\right) f_{a/n}(x,\mu^2)\right], \tag{2}$$

where Z is the charge and A the mass number of the nucleus. The CTEQ6M parametrization [34] for parton distribution functions will be used for nucleon parton distributions $f_{a/N}(x, \mu^2)$. The parton shadowing factor $S_{a/A}(x, \mu^2, \mathbf{r})$ describes the nuclear modification of parton distributions per nucleon inside a nucleus and can be given by parametrizations [35]. With an impact-parameter-dependent parton shadowing, the effect of shadowing is the strongest for hard scatterings at the center of the transverse plane. But partons from these hard scatterings at the center are mostly quenched due to parton energy loss and do not contribute to the final hadron spectra. Therefore, the effect of parton shadowing is negligible for the final hadron spectra in A+A collisions that are dominated by hard scattering close to the surface of the overlapping nuclei [36]. We will set $S_{a/A}(x, \mu^2, \mathbf{r})$=1.0 in the calculation. The effect of jet quenching in dense medium in heavy-ion collisions will be described by effective medium-modified parton fragmentation functions $\widetilde{D}^h_c(z_h, Q^2, E, b, r)$ within the HT approach.

Within the generalized factorization of twist-four processes, one can calculate the parton energy loss and medium-modified fragmentation functions of a propagating parton in the medium after it is produced via a hard process [37,38]. Within such a high-twist approach, the medium modification to the parton fragmentation functions is caused by multiple scattering inside the medium and induced gluon bremsstrahlung. The medium-modified quark fragmentation functions,

$$\tilde{D}^h_q(z_h,Q^2) = D^h_q(z_h,Q^2) + \frac{\alpha_s(Q^2)}{2\pi}\int_0^{Q^2}\frac{d\ell_T^2}{\ell_T^2} \times \int_{z_h}^1 \frac{dz}{z}\left[\Delta\gamma_{q\to qg}(z,\ell_T^2) D^h_q\left(\frac{z_h}{z}\right) + \Delta\gamma_{q\to gq}(z,\ell_T^2) D^h_g\left(\frac{z_h}{z}\right)\right], \tag{3}$$

take a form very similar to the vacuum bremsstrahlung corrections that lead to the evolution equations in pQCD for fragmentation functions, except that the medium-modified splitting functions, $\Delta\gamma_{q\to qg}(z, \ell_T^2)$ and $\Delta\gamma_{q\to gq}(z, \ell_T^2) = \Delta\gamma_{q\to qg}(1-z, \ell_T^2)$ depend on the properties of the medium via the jet transport parameter $\hat{q}$ [26,39],

$$\hat{q} = \rho \int dq_T^2 \frac{d\sigma}{dq_T^2} q_T^2. \tag{4}$$

or the average squared transverse momentum broadening per unit length, which is also related to the gluon distribution density of the medium [39,40]. The corresponding quark energy loss can be expressed as [26,39]

$$\frac{\Delta E}{E} = \frac{2N_c\alpha_s}{\pi}\int dy^-\, dz\, d\ell_T^2 \frac{1+z^2}{\ell_T^4} \times \left(1-\frac{1-z}{2}\right)\hat{q}(E,y)\sin^2\left[\frac{y^-\ell_T^2}{4Ez(1-z)}\right], \tag{5}$$

in terms of the jet transport parameter. Note that we include an extra factor of $1-(1-z)/2$ as compared to that used in Refs. [39,41] due to corrections beyond the helicity amplitude approximation [38]. We refer readers to Ref. [26] for details of the modified fragmentations. The fragmentation functions $D^0_{h/c}(z_c, \mu^2)$ in the vacuum are given by the updated AKK parametrization [42].

According to the definition of a jet transport parameter, we can assume it to be proportional to the local parton density in a QGP and hadron density in a hadronic gas. Therefore, in a dynamical evolving medium, one can express it in general as

$$\hat{q}(\tau,r) = \left[\hat{q}_0 \frac{\rho_{\rm QGP}(\tau,r)}{\rho_{\rm QGP}(\tau_0,0)}(1-f) + \hat{q}_h(\tau,r) f\right]\frac{p^\mu u_\mu}{p_0}, \tag{6}$$

where $\rho_{\rm QGP}$ is the parton (quarks and gluon) density in an ideal gas at a given temperature, $f(\tau, r)$ is the fraction of the hadronic phase at any given space and time, $\hat{q}_0$ denotes the jet transport parameter at the center of the bulk medium in the QGP phase at the initial time τ_0, p^μ is the four-momentum of the jet, and u^μ is the four flow velocity in the collision frame. We assume the hadronic phase of the medium is described as a hadron resonance gas, in which the jet transport parameter is approximated as

$$\hat{q}_h = \frac{\hat{q}_N}{\rho_N}\left[\frac{2}{3}\sum_M \rho_M(T) + \sum_B \rho_B(T)\right], \tag{7}$$

where ρ_M and ρ_B are the meson and baryon density in the hadronic resonance gas at a given temperature, respectively, $\rho_N = n_0 \approx 0.17\ \mathrm{fm}^{-3}$ is the nucleon density in the center of a large nucleus, and the factor 2/3 accounts for the ratio of constituent quark numbers in mesons and baryons. The jet transport parameter at the center of a large nucleus $\hat{q}_N$ has been studied in deeply inelastic scattering (DIS) [43–45]. We use a recently extracted value [41] $\hat{q}_N \approx 0.02\ \mathrm{GeV}^2/\mathrm{fm}$ from the HERMES [46] experimental data. The hadron density at a given temperature T and zero chemical potential is

$$\rho_h(T) = \frac{T^3}{2\pi^2}\left(\frac{m_h}{T}\right)^2 \sum_{n=1}^{\infty} \frac{\eta_h^{n+1}}{n} K_2\left(n\frac{m_h}{T}\right), \qquad (8)$$

where $\eta_h = \pm$ for meson (M)/baryon (B). In the paper, we will include all hadron resonances with mass below 1 GeV.

III. 3 + 1D IDEAL HYDRODYNAMIC EVOLUTION OF BULK MATTER

In the model for medium-modified fragmentation functions as described in the last section, one needs information on the space-time evolution of the local temperature and flow velocity in the bulk medium along the jet propagation path. We will use a full three-dimensional 3 + 1D ideal hydrodynamics [47,48] in our calculation to describe the space-time evolution of the bulk matter in heavy-ion collisions.

We solve equations of energy-momentum conservation in full 3 + 1D space (τ, x, y, η_s) under the assumption that local thermal equilibrium is reached at an initial time $\tau_0 = 0.6\ \mathrm{fm}/c$ and maintained thereafter until freeze-out. Here τ, η_s, x, and y are proper time, space-time rapidity, and two transverse coordinates perpendicular to the beam axis, respectively. Ideal hydrodynamics is characterized by the energy-momentum tensor,

$$T^{\mu\nu} = (\epsilon + P)u^\mu u^\nu - P g^{\mu\nu}, \qquad (9)$$

where ϵ, P, and u^μ are energy density, pressure, and local four-velocity, respectively. We neglect the finite net-baryon density which is supposed to be small both at RHIC and LHC energies. For the quark-gluon plasma (QGP) phase at high temperature ($T > T_c = 170$ MeV), we use the equation of state (EOS) of a relativistic massless parton gas (u, d, s quarks and gluons) with a bag pressure B:

$$p = \tfrac{1}{3}(\epsilon - 4B). \qquad (10)$$

The bag constant is tuned to be $B^{\frac{1}{4}} = 247$ MeV to match the pressure of the QGP phase to that of a hadron resonance gas at critical temperature $T_c = 170$ MeV. Below the critical temperature $T < T_c$, a hadron resonance gas model including all hadrons up to the mass of the $\Delta(1232)$ is employed for the EOS. The hadron resonance gas EOS employed in this study implements chemical freeze-out at $T_{\mathrm{ch}} = 170$ MeV [48] so that evolution of chemically frozen, but thermally equilibrated, hadronic matter is described. In the calculation of parton energy loss and medium-modified fragmentation functions, jets propagate along a straight path in the evolving medium until the decoupling of the medium at $T^{\mathrm{dec}} = 100$ MeV.

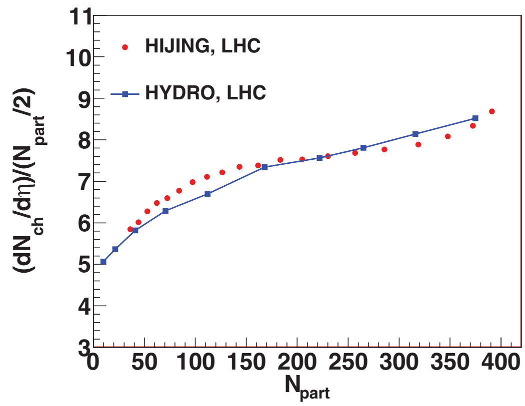

FIG. 1. (Color online) Charged particle multiplicity density at midrapidity per participant pair as a function of the number of participants in Pb+Pb collisions at $\sqrt{s_{NN}} = 2.76$ GeV from HIJING 2.0 (solid circles) [30] and ideal hydrodynamics (solid square).

For the initial condition of the longitudinal flow velocity, Bjorken's scaling solution [49] is employed. The initial entropy distribution in the transverse plane is proportional to a linear combination of the number density of participants, ρ_{part}, and that of binary collisions, ρ_{coll} [50]. The proportionality constant and the fraction of soft and hard components are so chosen that the centrality dependence of charged particle multiplicity agrees with the experimental data at RHIC [50] and HIJING2.0 results at the LHC energy [30] which agree with the recent ALICE data for the most central Pb+Pb collisions at $\sqrt{s} = 2.76$ TeV [28]. Shown in Fig. 1 is the hydrodynamic calculation (solid square) of the charged hadron multiplicity density at midrapidity as compared with the HIJING2.0 result (solid circle).

We will use these hydrodynamic solutions to provide values of temperature and flow velocity along the trajectory of parton propagation for the evaluation of local jet transport parameter in Eq. (6) for the calculation of medium-modified fragmentation functions. The hydrodynamic results obtained in this way such as temperature and energy density at each space-time position are publicly available [51]. Note that these hydrodynamic results provide the evolution of the space-time profiles of jet transport parameter and gluon density relative to their values at the center of overlapped region of dense matter ($r = 0$) in the most central collisions ($b = 0$) at an initial time τ_0. The normalization of the initial values at τ_0 and $r = 0, b = 0$ is included in the value of $\hat{q}_0$. It should be proportional to the initial parton density, which in turn is determined by fitting the final charged hadron multiplicity density in midrapidity (see Fig. 1) of the hydrodynamics results. Therefore, approximately,

$$\hat{q}_0 \propto \frac{1}{\pi\tau_0 R_A^2}\frac{dN_{\mathrm{ch}}}{d\eta}. \qquad (11)$$

We determine the coefficient of the above relation by fitting the experimental data at the RHIC energy for the most central Au+Au collisions. Then the energy dependence and the impact-parameter dependence will be completely determined by the measurement or calculated values of charged hadron multiplicity density $dN_{\mathrm{ch}}/d\eta$.

IV. NUMERICAL RESULTS

We use a NLO Monte Carlo based program [33] to calculate the single hadron spectra in our study. In this NLO program, the factorization scale and the renormalization scale are chosen to be the same (denoted as μ) and are all proportional to the transverse momentum of the final hadron p_T. As in all NLO pQCD parton model calculations, our calculated single inclusive pion spectra at large p_T in $p+p$ collisions depend on the choice of the factorization scale $\mu = 0.9p_T \sim 1.5p_T$, which is the intrinsic uncertainty in pQCD. We choose the scale $\mu = 1.2p_T$ with which the calculated π^0 spectra in $p+p$ collisions can fit RHIC data very well [17]. We use the same scale in $A+A$ collisions at both RHIC and LHC energies.

With space-time profile of the gluon density provided by the hydrodynamic evolution equations, we calculate medium-modified fragmentation functions which are used then to calculate the suppression factor (or nuclear modification factor) for large-p_T hadron spectra in heavy-ion collisions [52],

$$R_{AB} = \frac{d\sigma^h_{AB}/dy\, d^2p_T}{N^{AB}_{\rm bin}(b)d\sigma^h_{pp}/dy\, d^2p_T}, \quad (12)$$

where $N^{AB}_{\rm bin}(b) = \int d^2r t_A(r)t_B(|\vec{b}-\vec{r}|)$. The fixed value of impact parameters in the calculation of the spectra and the modification factor are determined through the Glauber geometric fractional cross sections for the given centrality of the heavy-ion collisions.

In the HT approach, we have determined $\hat{q}_0\tau_0 = 0.45$–$0.63\ \mathrm{GeV}^2$ from the experimental data on pion spectra in the most 0–10% central Au+Au collisions at $\sqrt{s} = 0.2$ TeV [26] as shown in Fig. 2 (red shaded curve). We assume that the jet transport parameter is proportional to the initial parton density or the transverse density of charged hadron multiplicity in midrapidity [Eq. (11)]. With the new ALICE data on charged particle pseudorapidity density at midrapidity $dN_{\rm ch}/d\eta = 1584 \pm 4(\mathrm{stat.}) \pm 76(\mathrm{sys.})$ [28] in the most central 5% Pb+Pb collisions at $\sqrt{s} = 2.76$ TeV versus $dN_{\rm ch}/d\eta = 687 \pm 37$ for 0–5% Au+Au collisions at $\sqrt{s} = 0.2$ TeV [53], we obtain the extrapolated value $\hat{q}_0\tau_0 = 1.0$–$1.4\ \mathrm{GeV}^2$ for Pb+Pb collisions at $\sqrt{s} = 2.76$ TeV. Shown in Fig. 2 (blue shaded curve) is the predicted nuclear modification factor for pion spectra in the 0–5% central Pb+Pb collisions at $\sqrt{s} = 2.76$ TeV. The suppression factor increases with p_T partially because of the energy dependence of parton energy loss and partially because of the less steep initial jet production spectra [54]. This trend is similar to almost all LHC predictions by many other parton energy loss model calculations [27].

We also show in Fig. 2 the recently published ALICE data [55] (filled square) on the suppression factor for charged hadrons in the most 0–5% central Pb+Pb collisions at the LHC energy $\sqrt{s} = 2.76$ TeV. Since there are no experimental data on charged hadron spectra in $p+p$ collisions at the LHC energy $\sqrt{s} = 2.76$ TeV, ALICE data on the suppression factor were obtained with $p+p$ spectra interpolated from experimental data at Tevatron energies. The histograms in Fig. 2 represent the errors on the suppression factor from the uncertainty in the interpolation. Within the $p_T < 20\ \mathrm{GeV}/c$, the suppression factor for charged hadrons at LHC energy $\sqrt{s} = 2.76$ TeV from the ALICE experiment is strikingly similar to that

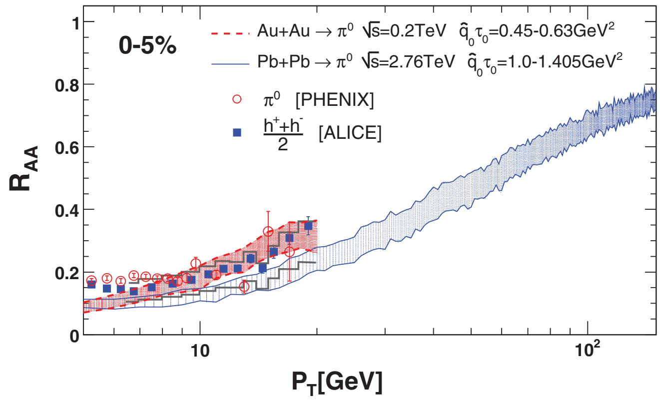

FIG. 2. (Color online) Nuclear modification factor at midrapidity for neutral pion spectra in the most 0–5% central Au+Au collisions at $\sqrt{s} = 0.2$ TeV (red dashed line) with $\hat{q}_0\tau_0 = 0.45$–$0.63\ \mathrm{GeV}^2$ and Pb+Pb collisions at $\sqrt{s} = 2.76$ TeV (blue solid line) with $\hat{q}_0\tau_0 = 1.0$–$1.4\ \mathrm{GeV}^2$, using the HT modified fragmentation functions. The data points are for π^0 (open circle) in the same central Au+Au collisions from PHENIX experiment [56] and charged hadrons (filled square) in Pb+Pb collisions from ALICE experiment [55] with the histogram representing systematic errors due to uncertainty in the $p+p$ spectra at $\sqrt{s} = 2.76$ TeV from interpolation.

for neutral pions at the RHIC energy $\sqrt{s} = 200$ GeV from the PHENIX experiment [56], which is, however, smaller than that for charged hadrons at the same RHIC energy. Charged hadrons contain significant fraction of protons and antiprotons which could have non-negligible contributions from parton recombination [57–59]. Because of the abundance of jet production at the LHC energy, recombination among these hard partons becomes possible and therefore contributes to hadron, especially baryon, spectra at high p_T. One therefore should take into account the contribution from hard parton recombination in the calculation of the final charged hadron spectra, which could push the suppression factor for charged hadrons higher than that for pions at large p_T.

Because of the increased initial parton density which we assume to be proportional to the final hadron multiplicity density, the initial jet transport parameter $\hat{q}_0$ in Pb+Pb collisions at the LHC energy $\sqrt{s} = 2.76$ TeV are more than twice larger than that in Au+Au collisions at the RHIC energy $\sqrt{s} = 0.2$ TeV. The hadron suppression factors in Pb+Pb collisions at LHC at moderate transverse momentum $p_T < 20\ \mathrm{GeV}/c$ are therefore about 50% smaller than that at RHIC [26], which we also show in Fig. 2 as the red dashed line. We also note that the p_T dependence of the suppression factor at RHIC is similar to that at LHC within the available range $p_T < 20$ GeV. Shown in Fig. 3 is the scaled jet transport parameter $\hat{q}(r,\tau)/\hat{q}(0,\tau_0)$ as a function of $\tau - \tau_0$ which is related to the parton and hadron density [Eq. (6)] as given by the hydrodynamic evolution. The kink in the time dependence is caused by the first-order phase transition assumed in the hydrodynamics evolution as the EOS of the dense matter. For most part of the evolution history, the scaled jet transport parameters are very similar at RHIC and LHC energies. Therefore, the increased hadron suppression at LHC energies

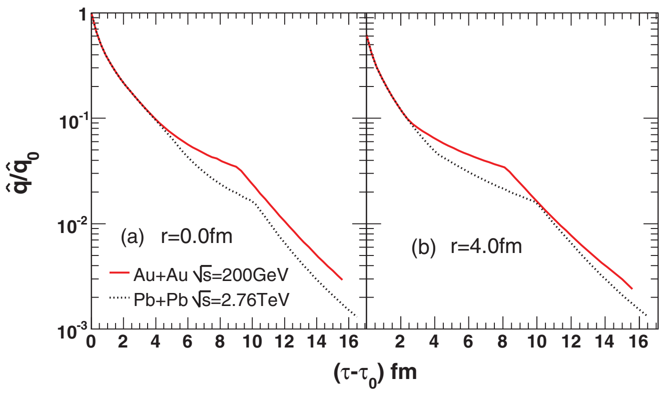

FIG. 3. (Color online) Scaled jet transport parameter $\hat{q}(r,\tau)/\hat{q}(0,\tau_0)$ as a function of $\tau-\tau_0$ at $r=0$ and $r=4$ fm in central Au+Au collisions at RHIC ($\sqrt{s}=0.2$ TeV) and Pb+Pb collisions at LHC ($\sqrt{s}=2.76$ TeV) from 3 + 1D hydrodynamic evolution.

is caused mainly by the overall increase of the initial parton density. The increased initial parton density, however, will also increase the lifetime of the dense matter throughout the phase transition and hadronic phase. This will also contribute to the increased suppression of hadron spectra at the LHC as compared to RHIC energies.

V. CONCLUSIONS

We used the new ALICE data on charged hadron multiplicity density at midrapidity in central Pb+Pb collisions at the LHC energy $\sqrt{s}=2.76$ TeV [28] to estimate the initial jet quenching parameters in Pb+Pb collisions at the LHC and the initial condition for the hydrodynamic evolution of the bulk matter. With the initial values of the jet transport parameter and the initial condition for hydrodynamic evolution of the bulk matter, we predict the suppression factor for the hadron spectra in Pb+Pb collisions at $\sqrt{s}=2.76$ TeV within the HT model for medium-modified fragmentation functions. Because of the increased initial parton density of about a factor of 2, and the longer lifetime of the dense matter or the duration of jet quenching, the hadron spectra are found to be suppressed more at LHC than at RHIC energies. Because the energy dependence of the parton energy loss and the less steep initial jet spectra, the suppression factors will increase with p_T at LHC energies. Coincidentally, the p_T dependence of the suppression factor at the RHIC energy is similar to that at LHC within the available $p_T < 20$ GeV range.

Because of the increased number of jet production in heavy-ion collisions at LHC energies, there is an increased possibility of larger-p_T hadron production from the recombination of parton showers from independent jets. This production mechanism will be more important than the shower-thermal and thermal-thermal parton recombinations that have been considered more relevant in heavy-ion collisions at RHIC energies [57–59]. Such contributions from a jet-jet parton recombination will likely increase the hadron yield at moderate p_T and increase the values of the suppression factor R_{AA} at LHC energies.

ACKNOWLEDGMENTS

This work was supported by NSFC of China under Projects No. 10825523 and No. 10875052 and Key Grant No. 11020101060, and by MOE and SAFEA of China under Project No. PITDU-B08033, and by Key Laboratory of Quark & Lepton Physics (Huazhong Normal University) of MOE of China under Project No. QLPL200913, and by the Director, Office of Energy Research, Office of High Energy and Nuclear Physics, Divisions of Nuclear Physics, of the U.S. Department of Energy under Contract No. DE-AC02-05CH11231 and with the framework of the JET Collaboration, and Grant-in-Aid for Scientific Research No. 22740151 and through the Excellent Young Researchers Overseas Visit Program (No. 213383) of the Japan Society for the Promotion of Science. T.H. thanks members of the Nuclear Theory Program at Lawrence Berkeley National Laboratory for kind hospitality during his sabbatical stay.

[1] I. Arsene *et al.* (BRAHMS Collaboration), Nucl. Phys. A **757**, 1 (2005).
[2] B. B. Back *et al.*, Nucl. Phys. A **757**, 28 (2005).
[3] J. Adams *et al.* (STAR Collaboration), Nucl. Phys. A **757**, 102 (2005).
[4] K. Adcox *et al.* (PHENIX Collaboration), Nucl. Phys. A **757**, 184 (2005).
[5] X. N. Wang and M. Gyulassy, Phys. Rev. Lett. **68**, 1480 (1992).
[6] J. Adams *et al.* (STAR Collaboration), Phys. Rev. Lett. **91**, 072304 (2003); **91**, 172302 (2003).
[7] S. S. Adler *et al.* (PHENIX Collaboration), Phys. Rev. Lett. **91**, 072301 (2003).
[8] C. Adler *et al.*, Phys. Rev. Lett. **90**, 082302 (2003).
[9] X.-N. Wang, Z. Huang, and I. Sarcevic, Phys. Rev. Lett. **77**, 231 (1996).
[10] A. Adare *et al.* (PHENIX Collaboration), Phys. Rev. C **80**, 024908 (2009).
[11] B. I. Abelev *et al.* (STAR Collaboration), Phys. Rev. C **82**, 034909 (2010).
[12] X. -N. Wang, Nucl. Phys. A **750**, 98 (2005).
[13] I. Vitev and M. Gyulassy, Phys. Rev. Lett. **89**, 252301 (2002).
[14] X. N. Wang, Phys. Lett. B **595**, 165 (2004).
[15] K. J. Eskola, H. Honkanen, C. A. Salgado, and U. A. Wiedemann, Nucl. Phys. A **747**, 511 (2005).
[16] T. Renk, Phys. Rev. C **74**, 024903 (2006).
[17] H. Zhang, J. F. Owens, E. Wang, and X. N. Wang, Phys. Rev. Lett. **98**, 212301 (2007).
[18] G. Y. Qin, J. Ruppert, C. Gale, S. Jeon, G. D. Moore, and M. G. Mustafa, Phys. Rev. Lett. **100**, 072301 (2008).
[19] T. Renk, Phys. Rev. C **74**, 034906 (2006).

[20] H. Zhang, J. F. Owens, E. Wang, and X.-N. Wang, Phys. Rev. Lett. **103**, 032302 (2009).
[21] G. Y. Qin, J. Ruppert, C. Gale, S. Jeon, and G. D. Moore, Phys. Rev. C **80**, 054909 (2009).
[22] M. Gyulassy *et al.*, in *Quark-Gluon Plasma 3*, edited by R. C. Hwa and X.-N. Wang (World Scientific, Singapore, 2004), p. 123.
[23] A. Kovner, U. A. Wiedemann, in *Quark-Gluon Plasma 3*, edited by R. C. Hwa and X.-N. Wang (World Scientific, Singapore, 2004), p. 192.
[24] S. A. Bass, C. Gale, A. Majumder, C. Nonaka, G. Y. Qin, T. Renk, and J. Ruppert, Phys. Rev. C **79**, 024901 (2009).
[25] N. Armesto, M. Cacciari, T. Hirano, J. L. Nagle, and C. A. Salgado, J. Phys. G **37**, 025104 (2010).
[26] X. -F. Chen, C. Greiner, E. Wang, X.-N. Wang, and Z. Xu, Phys. Rev. C **81**, 064908 (2010).
[27] N. Armesto *et al.*, J. Phys. G **35**, 054001 (2008).
[28] K. Aamodt *et al.* (The ALICE Collaboration), Phys. Rev. Lett. **105**, 252301 (2010).
[29] S. -Y. Li and X. -N. Wang, Phys. Lett. B **527**, 85 (2002).
[30] W. -T. Deng, X. -N. Wang, and R. Xu, Phys. Rev. C **83**, 014915 (2011).
[31] X. -N. Wang and M. Gyulassy, Phys. Rev. D **44**, 3501 (1991).
[32] W. T. Deng, X. N. Wang, and R. Xu, Phys. Lett. B **701**, 133 (2011).
[33] N. Kidonakis and J. F. Owens, Phys. Rev. D **63**, 054019 (2001); B. W. Harris and J. F. Owens, *ibid.* **65**, 094032 (2002).
[34] H. L. Lai *et al.* (CTEQ Collaboration), Eur. Phys. J. C **12**, 375 (2000).
[35] K. J. Eskola, H. Paukkunen, and C. A. Salgado, J. High Energy Phys. 07 (2008) 102.
[36] See contribution by H.-Z. Zhang, E. Wang, and X.-N. Wang in Ref. [27].
[37] X. F. Guo and X. N. Wang, Phys. Rev. Lett. **85**, 3591 (2000); X. N. Wang and X. F. Guo, Nucl. Phys. A **696**, 788 (2001).
[38] B. W. Zhang and X. N. Wang, Nucl. Phys. A **720**, 429 (2003).
[39] J. Casalderrey-Solana and X. N. Wang, Phys. Rev. C **77**, 024902 (2008).
[40] R. Baier, Y. L. Dokshitzer, A. H. Mueller, S. Peigne, and D. Schiff, Nucl. Phys. B **484**, 265 (1997).
[41] W. T. Deng and X. N. Wang, Phys. Rev. C **81**, 024902 (2010).
[42] S. Albino, B. A. Kniehl, and G. Kramer, Nucl. Phys. B **803**, 42 (2008).
[43] E. Wang and X. N. Wang, Phys. Rev. Lett. **89**, 162301 (2002).
[44] A. Majumder, E. Wang, and X. N. Wang, Phys. Rev. Lett. **99**, 152301 (2007).
[45] A. Majumder, arXiv:0901.4516 [nucl-th].
[46] A. Airapetian *et al.* (HERMES Collaboration), Nucl. Phys. B **780**, 1 (2007).
[47] T. Hirano, Phys. Rev. C **65**, 011901 (2001).
[48] T. Hirano and K. Tsuda, Phys. Rev. C **66**, 054905 (2002).
[49] J. D. Bjorken, Phys. Rev. D **27**, 140 (1983).
[50] T. Hirano, U. Heinz, D. Kharzeev, R. Lacey, and Y. Nara, Phys. Lett. B **636**, 299 (2006); Phys. Rev. C **77**, 044909 (2008).
[51] [http://tkynt2.phys.s.u-tokyo.ac.jp/hirano/parevo/parevo.html].
[52] X. N. Wang, Phys. Rev. C **61**, 064910 (2000).
[53] K. Adcox *et al.* (PHENIX), Phys. Rev. Lett. **86**, 3500 (2001).
[54] X. N. Wang, Phys. Rev. C **70**, 031901 (2004).
[55] K. Aamodt *et al.* (ALICE Collaboration), Phys. Lett. B **696**, 30 (2011).
[56] A. Adare *et al.* (PHENIX Collaboration), Phys. Rev. Lett. **101**, 232301 (2008).
[57] R. C. Hwa and C. B. Yang, Phys. Rev. C **67**, 034902 (2003).
[58] V. Greco, C. M. Ko, and P. Levai, Phys. Rev. Lett. **90**, 202302 (2003).
[59] R. J. Fries, B. Müller, C. Nonaka, and S. A. Bass, Phys. Rev. Lett. **90**, 202303 (2003).